NASA/TM–20210021062

A Straightforward Approach to Thickness Tailoring in Composite Structures Using Non-traditional Layups

W.E. Guin and A.T. Nettles
Marshall Space Flight Center, Huntsville, Alabama

November 2021

The NASA STI Program…in Profile

Since its founding, NASA has been dedicated to the advancement of aeronautics and space science. The NASA Scientific and Technical Information (STI) Program Office plays a key part in helping NASA maintain this important role.

The NASA STI Program Office is operated by Langley Research Center, the lead center for NASA's scientific and technical information. The NASA STI Program Office provides access to the NASA STI Database, the largest collection of aeronautical and space science STI in the world. The Program Office is also NASA's institutional mechanism for disseminating the results of its research and development activities. These results are published by NASA in the NASA STI Report Series, which includes the following report types:

- TECHNICAL PUBLICATION. Reports of completed research or a major significant phase of research that present the results of NASA programs and include extensive data or theoretical analysis. Includes compilations of significant scientific and technical data and information deemed to be of continuing reference value. NASA's counterpart of peer-reviewed formal professional papers but has less stringent limitations on manuscript length and extent of graphic presentations.

- TECHNICAL MEMORANDUM. Scientific and technical findings that are preliminary or of specialized interest, e.g., quick release reports, working papers, and bibliographies that contain minimal annotation. Does not contain extensive analysis.

- CONTRACTOR REPORT. Scientific and technical findings by NASA-sponsored contractors and grantees.

- CONFERENCE PUBLICATION. Collected papers from scientific and technical conferences, symposia, seminars, or other meetings sponsored or cosponsored by NASA.

- SPECIAL PUBLICATION. Scientific, technical, or historical information from NASA programs, projects, and mission, often concerned with subjects having substantial public interest.

- TECHNICAL TRANSLATION. English-language translations of foreign scientific and technical material pertinent to NASA's mission.

Specialized services that complement the STI Program Office's diverse offerings include creating custom thesauri, building customized databases, organizing and publishing research results…even providing videos.

For more information about the NASA STI Program Office, see the following:

- Access the NASA STI program home page at <http://www.sti.nasa.gov>

- E-mail your question via the Internet to <help@sti.nasa.gov>

- Phone the NASA STI Help Desk at 757–864–9658

- Write to:
  NASA STI Information Desk
  Mail Stop 148
  NASA Langley Research Center
  Hampton, VA 23681–2199, USA

NASA/TM–20210021062

A Straightforward Approach to Thickness Tailoring in Composite Structures Using Non-traditional Layups

W.E. Guin and A.T. Nettles
Marshall Space Flight Center, Huntsville, Alabama

National Aeronautics and
Space Administration

Marshall Space Flight Center • Huntsville, Alabama 35812

November 2021

Acknowledgments

The authors thank Dawn Price (NASA MSFC), Michelle Rudd (NASA MSFC), and Stephen Tsai (Stanford University) for the many helpful discussions on this topic.

TRADEMARKS

Available from:

NASA STI Information Desk
Mail Stop 148
NASA Langley Research Center
Hampton, VA 23681–2199, USA
757–864–9658

This report is also available in electronic form at
<http://www.sti.nasa.gov>

TABLE OF CONTENTS

LIST OF FIGURES

LIST OF FIGURES (Continued)

LIST OF TABLES

LIST OF ACRONYMS

2D	two dimensional
CG	center of gravity
CLT	classic lamination theory
DOF	degree of freedom
FEA	finite element analysis
FPF	first ply failure
KCC	kinematic coupling constraint
KDF	knockdown factor
NCAMP	National Center for Advanced Materials Performance
NESC	NASA Engineering and Safety Center
NIAR	National Institute for Aviation Research
PMC	polymer matrix composites
SBKF	shell buckling knockdown factor
WWFE	Worldwide Failure Exercise

NOMENCLATURE

f^*	cross-product term coefficient
F^*_{xy}	cross-product term coefficient
M	overturning moment
MS	margin of safety
N_p	equivalent line load
P	axial load
P_{eq}	equivalent maximum axial load
R	strength ratio
$R_{nominal}$	nominal radius
SF	safety factor
t	shell thickness
ε_i	local strains
$\lambda_{buckling}$	eigenvalues
σ_i	local stresses

TECHNICAL MEMORANDUM

A STRAIGHTFORWARD APPROACH TO THICKNESS TAILORING IN COMPOSITE STRUCTURES USING NON-TRADITIONAL LAYUPS

1. INTRODUCTION

1.1 Background

One of the primary benefits offered when using polymer matrix composites (PMCs) is tailorability. The ability to tune performance characteristics by manipulating composite layups can provide a unique opportunity to tailor a given structure precisely for the application at hand. However, real-world constraints often dictate that this tailorability is difficult to fully realize in practice. Design requirements are rarely firm in the initial stages of a project. As such, minimization of risk is often a principal concern in the preliminary sizing process. This influences decision making toward material systems and composite layups with pedigree as well as conservative safety and knockdown factors. While the commonly adopted iterative approach to design and analysis provides for eventual refinement of previously selected design concepts, the influences of cost, schedule, and risk can restrict the degree to which this design refinement is ultimately carried out. As a result, the benefits of tailorability offered by PMCs are often underutilized.

In flight-hardware applications where structures must be rigorously qualified, tailoring can bring about challenges with respect to design substantiation. While 'tailoring' can generally refer to laminate thickness tailoring and/or fiber angle tailoring, this study is primarily focused on laminate thickness tailoring. Each distinct composite layup family in a given structure likely warrants some level of characterization. While the qualification process often starts at the lamina level, layup-specific properties should ultimately be considered. This is particularly true for strength-based properties, as lamina-level analyses alone, though useful in the initial stages of a project, are not ideal for final design substantiation.[1] However, the development of layup-specific properties for the purposes of design substantiation is a cost- and time-intensive process. Thus, minimizing the number of composite layup families to be characterized (which is inherently difficult to achieve where tailoring is desired) is often imperative.

In approaching this issue, two concepts in particular are worth considering in detail. The first is the layup family concept. For the purposes of this study, a layup family is designated as a class of composite layups that share the same or exceedingly similar laminate-level properties across a range of ply counts/laminate thicknesses. For a given layup configuration to remain in-family per this designation, layup composition (i.e., 25% 0° plies, 50% ±45° plies, and 25% 90° plies in a [+45/0/–45/90] quasi-isotropic layup), balance, and symmetry must be maintained as plies are

added or removed. The relative significance of these three components (layup composition, balance, and symmetry) can vary with layup family and should be evaluated on a case-by-case basis.

The second concept worth considering in detail is effective repeating unit size. The effective repeating unit is designated as the ply or group of plies that must be added or removed in the thickness tailoring process to keep a laminate in-family. A smaller effective repeating unit provides greater potential for laminate thickness tailoring. Therefore, minimizing the effective repeating unit size can be equated to improving the fidelity with which thickness tailoring can be carried out. Thus, non-traditional layups where effective repeating unit size can be minimized should be considered.

1.2 Non-traditional Layups

Double-biaxial angle layups ($[\pm\theta/\pm\Psi]$ in their most general form) offer an opportunity to minimize effective repeating unit size, as claimed by Tsai, et al.[2,3] As previously mentioned, opportunities for thickness tailoring are much more accessible where a minimal number of plies can be readily added or removed without invalidating laminate properties. This allows an iterative design and analysis approach to function more effectively via the ability to refine and optimize composite layups over the course of a project.

Among double bi-axial angle layups, the case where $\theta = \Psi$ (written from this point forward as $[\pm\theta]$) is particularly useful in practice, given that $[\pm\theta]$ layups are naturally well-suited for thickness tailoring. Given the considerations previously discussed with respect to maintaining in-family laminates in the thickness tailoring process, several $[\pm\theta]$ layup configurations were considered relative to a baseline 4-ply $[\pm\theta]$ layup. Elastic properties and Tsai-Wu first ply failure (FPF) strengths were determined for each. Figures 1 and 2 show these layup configurations and accompanying laminate-level property evaluations.

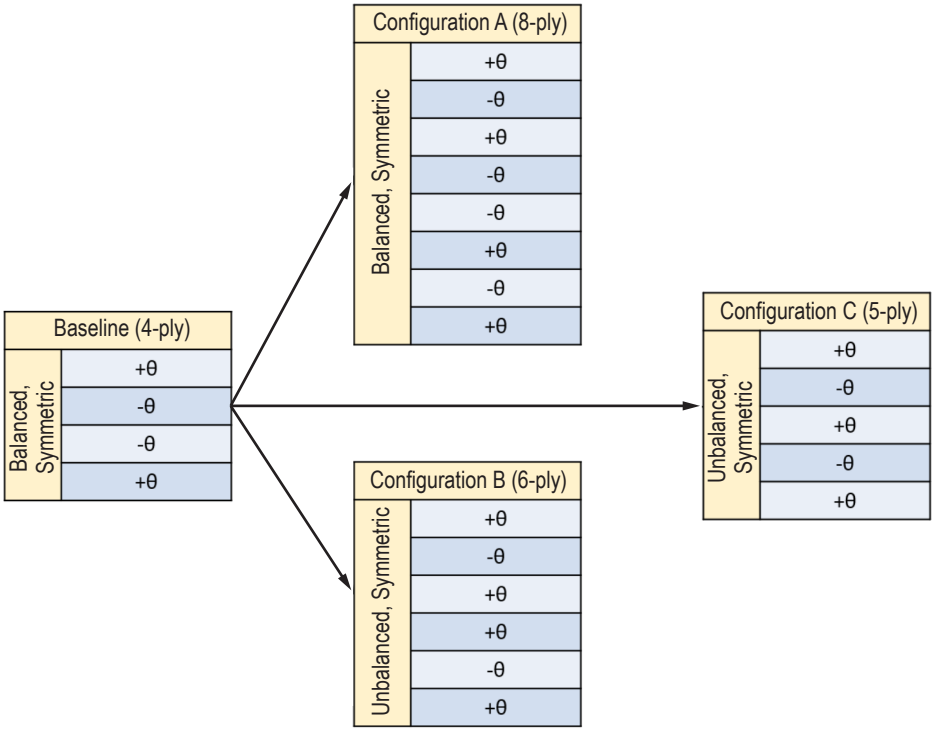

Figure 1. Layup configurations considered for [±θ] layup evaluations.

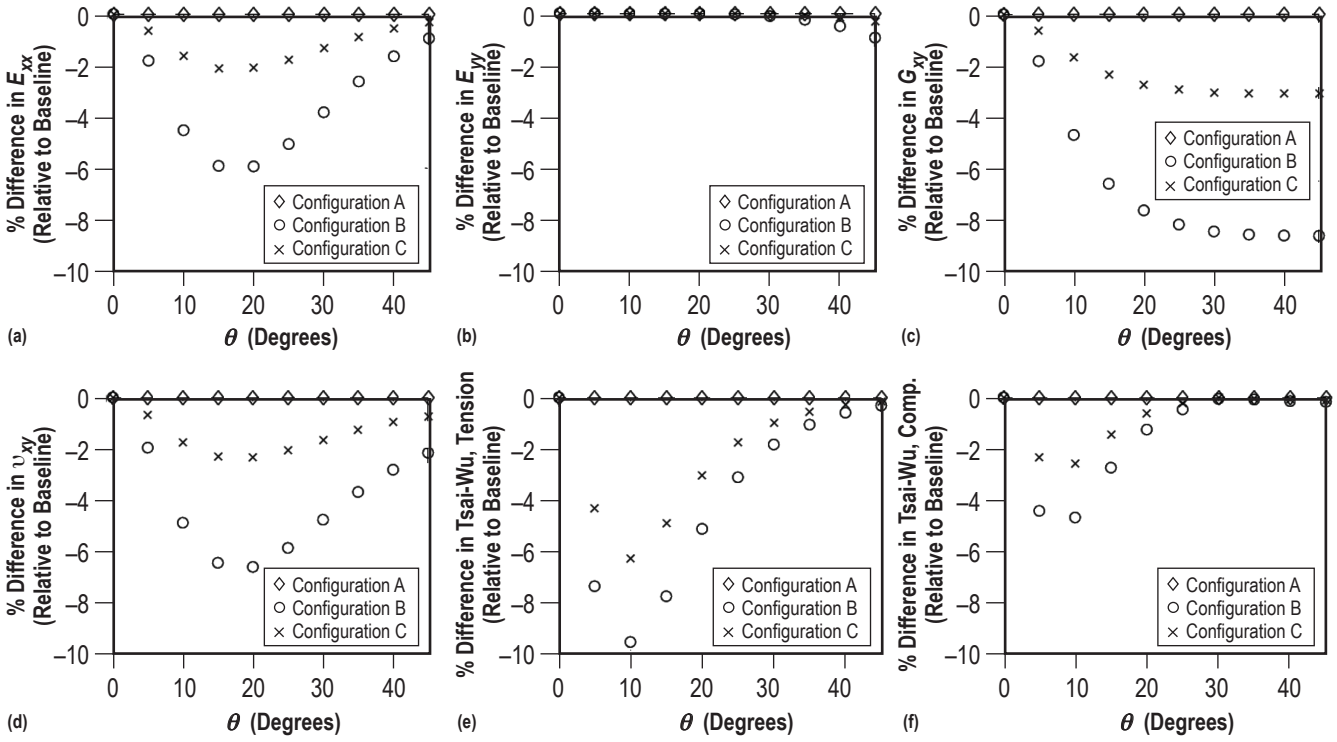

Figure 2. [±θ] Layup evaluations with comparisons among the layup configurations shown in Figure 1 for: (a) E_{xx}, (b) E_{yy}, (c) G_{xy}, (d) v_{xy}, (e) Tsai-Wu FPF stresses in tension, and (f) Tsai-Wu FPF stresses in compression.

As shown in Figure 2, classical lamination theory (CLT) and the Tsai-Wu failure criterion predict that balance and symmetry can have a significant effect on laminate-level properties in [±θ] layups. While layup composition is maintained in each of the three layup configurations, only configuration A, where balance and symmetry are also maintained, provides for unchanged laminate-level properties regardless of the value of . Thus, thickness tailoring with [±θ] layups entails an effective repeating unit size of 4 plies. In contrast, effective repeating unit size for a [+45/0/–45/90] quasi-isotropic layup is 8 plies (where layup composition, balance, and symmetry are maintained). As such, [±θ] layups provide an opportunity for improved fidelity in the thickness tailoring process.

1.3 Case Study Overview

To evaluate the potential of [±θ] layups in the context of a large-scale composite structure, a case study has been developed and carried out. A large-scale, adapter-type structure was considered due to its relevancy in a wide range of applications in launch vehicle structures as well as its potential for tailorability (given the frustum geometry). The structure was modeled using the commercially available finite element analysis (FEA) software Abaqus™. An overview of the structure considered herein is shown in Figure 3.

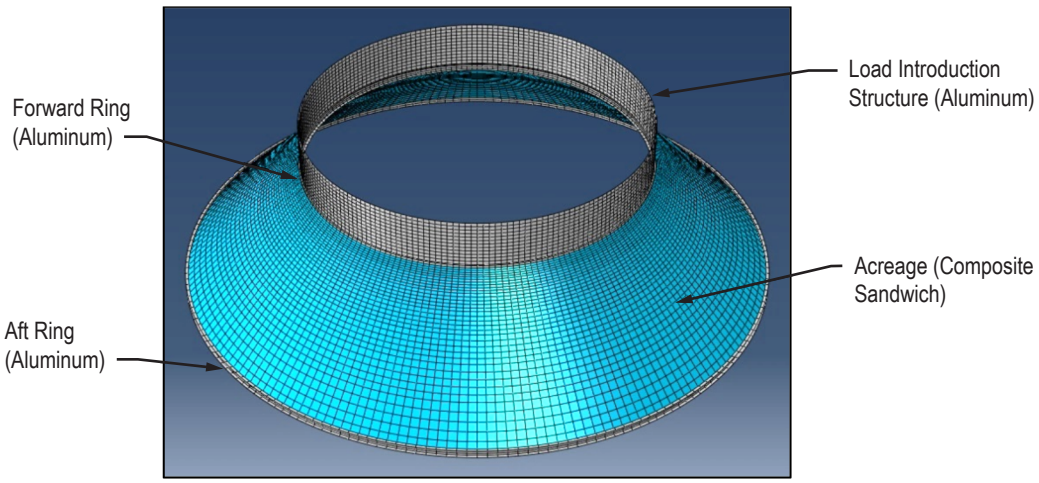

Figure 3. Overview of adapter considered in the case study (aluminum components shown in gray, composite sandwich acreage shown in blue).

Primary structural components include the acreage (composite sandwich), circumferential rings at the forward and aft ends (aluminum), and a cylindrical load introduction structure (aluminum). Generic geometries (most notably, 15-ft forward diameter, 25-ft aft diameter, and 45° cone angle) and widely used material systems (most notably, IM7/8552 for composite facesheets) were considered. Using a [±θ] layup, the composite facesheets were tailored in view of typical strength and buckling requirements. Adapter weight was estimated for each of the tailored configurations in order to evaluate weight savings potential associated with this approach.

2. METHODOLOGY

2.1 Material Properties and Model Definitions

Widely used material systems (for which material properties are readily available) were considered in the case study presented herein. For the composite sandwich structure, IM7/8552 (unidirectional, 190 gsm, 35% resin content) was considered for the facesheets while traditional aluminum honeycomb core (5056 alloy, 4.5 pcf, 0.125-in cells, 1-in thick) was considered for the core. For the aluminum structural sections, 7075-T6 alloy was considered. Note that the primary focus of this study is the composite sandwich acreage, and as such, performance of the aluminum structural sections was not given particular attention beyond basic model checks.

IM7/8552 composite facesheets were modeled as orthotropic lamina and layups were defined via the composite layup editor in Abaqus. Material properties were taken from the database generated by the National Center for Advanced Materials Performance (NCAMP) and the National Institute for Aviation Research (NIAR).[4] In particular, lamina-level properties were leveraged, given that a wide range of composite-facesheet layups were considered herein. For elastic properties, average values (between tension and compression values) were used for strength and natural frequency analyses while compression values were used for linear buckling analyses. This practice is consistent with the guidelines detailed in CMH-17, Revision G, Volume 3, Section 8.3.3.[5] Note that the elastic properties considered herein are mean values. Since through-the-thickness shear modulus values for IM7/8552 are neither readily available nor a significant influence in the context of thin composite facesheets, these values have been approximated as equivalent to in-plane shear modulus in order to populate the orthotropic lamina material definition in Abaqus. Table 1 shows the elastic properties considered for IM7/8552.

Table 1. IM7/8552 elastic properties.

Input Values	E_{11} (Msi)	E_{22} (Msi)	ν_{12}	G_{12} (Msi)	G_{13} (Msi)	G_{23} (Msi)
Tension	22.99	1.30	0.316	0.68	0.68†	0.68†
Compression	20.04	1.41	0.356	0.68	0.68†	0.68†
Average	21.52	1.36	0.336	0.68	0.68†	0.68†

† Value not readily available and is approximated to facilitate material definition in FEA; not a significant influence in analyses.

For strength properties, lamina-level B-basis allowables were considered where stress-based failure theories were used. Table 2 shows the material properties considered for stress-based failure in IM7/8552. Note that the NCAMP/NIAR database does not report a B-basis value for lamina compression strength in the fiber direction. As such, a Monte-Carlo basis value simulation code previously developed by the authors[1] was used to estimate this value using the summary statistics (mean and coefficient of variation) available in the NCAMP/NIAR database.

Table 2. IM7/8552 material property values for stress-based failure theories.

Input Values (ksi)	X_T	Y_T††	S	X_C	Y_C
B-basis	323.09	7.59	6.87	215.25‡	36.45

†† Lamina-level test for transverse tension strength does not yield an intrinsic material property; see ref. [6] for details.

‡ Value not reported in NCAMP/NIAR database. Value shown is estimated via Monte-Carlo basis value simulation code.

Aluminum honeycomb core was also modeled as an orthotropic lamina and was incorporated in sandwich configurations via the composite layup editor in Abaqus (with ribbon direction of core aligned with 0° fiber direction). Out-of-plane shear moduli were taken from Hexcel®'s product data sheet for HexWeb® aluminum honeycomb core materials.[7] In-plane elastic properties (moduli and Poisson's ratio) for the core material are not a significant influence in the analyses carried out herein; these values have been approximated per Gibson and Ashby's approach for equivalent elastic properties in honeycomb materials (Table 3).[8,9]

Table 3. Aluminum honeycomb core (5056 alloy, 4.5 pcf, 0.125-in cells) elastic properties.

Input Values	E_{11} (ksi)	E_{22} (ksi)	v_{12}	G_{12} (ksi)	G_{13} (ksi)	G_{23} (ksi)
Mean	0.06‡‡	0.06‡‡	0.995‡‡	.015‡‡	70	28

‡‡ Values approximated per [8,9]; not a significant influence in analyses carried out herein.

Structural sections made of 7075-T6 aluminum were modeled as isotropic. Commonly available material properties for this alloy were used: 10.4 Msi for elastic modulus and 0.33 for Poisson's ratio. Forward and aft rings were modeled as C-channels (4-in web, 1.5-in flanges, 0.75-in thick), while the load introduction structure (24-in tall) was modeled as a constant thickness (1-in thick) cylinder.

The adapter was modeled in FEA using conventional shell elements. In particular, S4R elements were used (4-node doubly curved thin shells with reduced integration, hourglass control, and finite membrane strains).

2.2 Boundary Conditions and Applied Loads

A displacement-type boundary condition was applied to the lower flange of the aft ring, where degrees of freedom (DOFs) 1–6 were constrained (i.e., translations and rotations fixed). Compared to the application of the aft end boundary condition, the selection and application of loads was a less straightforward process. Given typical use cases for adapters, such as the one considered herein, a single load case dominated by a compressive axial (vertical) load applied to the forward end was considered in this study. In lieu of individual applied axial and lateral loads, an equivalent maximum axial load, P_{eq}, was used to represent this collection of loads with a single applied load. This approach is commonly taken,[10,11,12] and is particularly useful in preliminary sizing for axisymmetric structures as it provides for coverage with respect to design and analysis

where the location of structural features (such as joints, cut outs, attachment points, etc.) has not yet been defined. In addition to the equivalent maximum axial load, a uniform crush pressure was applied to the composite sandwich acreage.

With respect to load introduction, a simple cylinder of uniform thickness (1 in) comprised of 7075-T6 aluminum was used above the top flange of the forward ring. This approach was taken to provide a buffer between the applied load and the structure itself. As shown in Figure 4, the equivalent maximum axial load, P_{eq}, was applied via a reference point and an accompanying kinematic coupling constraint (KCC). The reference point was placed above the forward end of the load introduction structure and centered within the load introduction structure/adapter. The equivalent maximum axial load was applied to the reference point and a KCC was used to couple the reference point to the forward end of the load introduction structure. DOFs 1–6 were coupled in this case; that is, the nodes along the forward end of the load introduction structure were constrained in all three translational and all three rotational DOFs to the rigid body motion of the single node at the reference point. While the KCC effectively rigidized the forward end of the load introduction structure, the load introduction structure provided some degree of compliance between the applied load and the adapter. In flight-hardware applications, load introduction would typically be carefully modeled, and in a full-scale test scenario, simulated via appropriate test hardware, in order to mimic real-world interactions between applied loads and the structure of interest as closely as possible. The generic approach described in this section was taken in an effort to introduce loads into the adapter in an adequate manner, all the while recognizing that load introduction is often application-specific and can vary widely in practice.

A maximum equivalent axial load, P_{eq}, was developed for a 75 t (165,347 lbf) payload with a center of gravity (CG) located 60 in above the forward end of the load introduction structure (with no lateral CG offset). Equivalent axial and lateral accelerations of 3.50 g were considered. The conventional equation for thin shell axisymmetric structures loaded with an axial force and overturning moment was used to develop P_{eq} for this application:

$$P_{eq} = P \pm \frac{2M}{R_{nominal}} \tag{1}$$

where

P = axial load
M = overturning moment
$R_{nominal}$ = nominal radius at the forward end of the structure.

Equation (1) is derived in app. B.

For the adapter considered in this study, a P_{eq} value of 1,356,814 lbf was calculated using equation (1). Note that in this case, the critical P_{eq} value resulted from adding (rather than subtracting) the axial load and overturning moment terms. As previously mentioned, a uniform crush pressure (i.e., pressure applied from outside of structure toward inside of structure) of 0.1 psi was applied to the composite sandwich acreage. While magnitude and direction will vary with

application, this accounts for a differential pressure that can develop between the inner and outer volumes of the adapter. Figure 4 summarizes the loads and boundary conditions considered in this study.

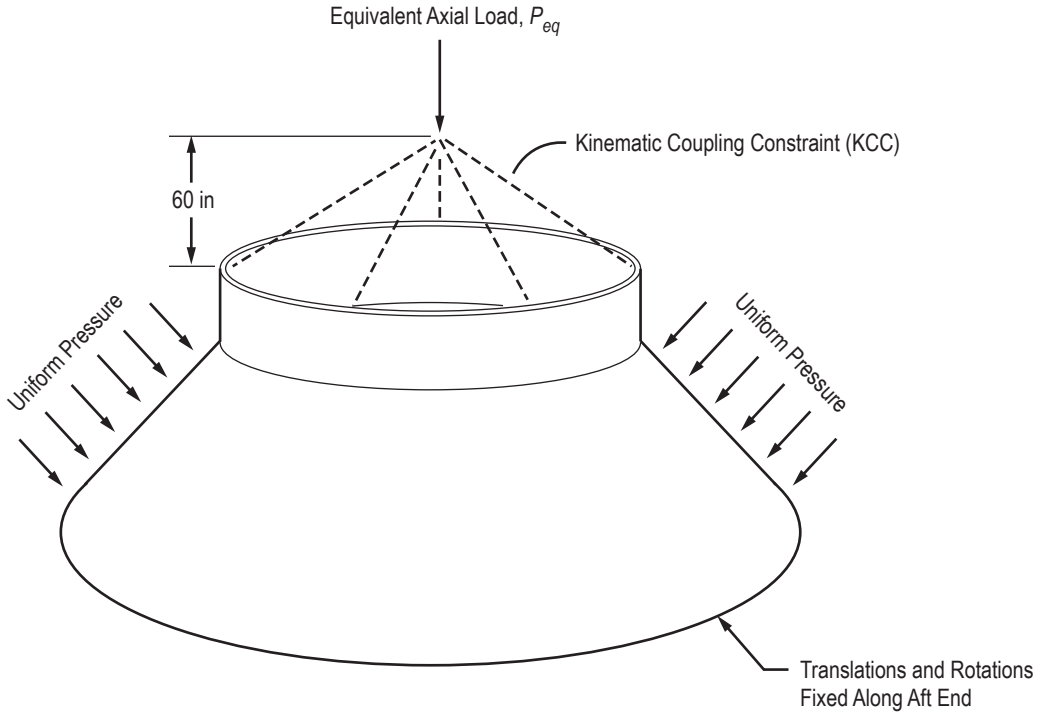

Figure 4. Overview of loads and boundary conditions considered for the adapter in this study.

Note that the reference point used for load application was placed at 60 in above the forward end to coincide with the physical location of the payload CG. This was done purely as a matter of preference, since an axial CG offset has no influence in this situation where only axial load was applied to the reference point.

2.3 Strength Analysis

Failure prediction in multi-directional composite laminates is notoriously challenging. This issue has been well-documented over the years, perhaps most notably through the Worldwide Failure Exercise (WWFE),[13] which evaluated a wide range of composites failure theories in an objective manner and included many of the leading experts in the field (with the notable exception of Hashin[14]). The WWFE highlighted the shortcomings of many predictive failure theories for composites, which can largely be attributed to the inherent difficulty in accurately modeling the complex damage processes known to occur prior to and during a failure event. However, the need for analytical tools to aid in the design process (especially early on) dictates that these failure theories, despite their known shortcomings, must be relied upon to some extent. Ply-by-ply approaches offer considerable flexibility in the layup development/selection process, as lamina-level properties can be used preliminarily to evaluate any number of layup configurations.

Given these considerations, several ply-by-ply failure theories were considered in this study, including Tsai-Wu, Tsai-Hill, and Maximum Stress (each assuming first ply failure with no progressive damage to provide for quick-turnaround model runs). Note that a value of –0.5 was used for the interaction term (also known as cross product term coefficient; commonly written as F^*_{xy} or f^*) for Tsai-Wu failure calculations. Along with these traditionally considered failure theories, a failure theory recently introduced by Stephen Tsai—Nettles Circle—was also considered. Shown graphically in Figure 5, Nettles Circle is a special case of the unit circle failure criterion[2,15,16] where a single strain value is used to define limits for principal strains regardless of loading direction or coordinate system rotation. This is based on the common practice of implementing a cutoff strain in composites design and analysis.

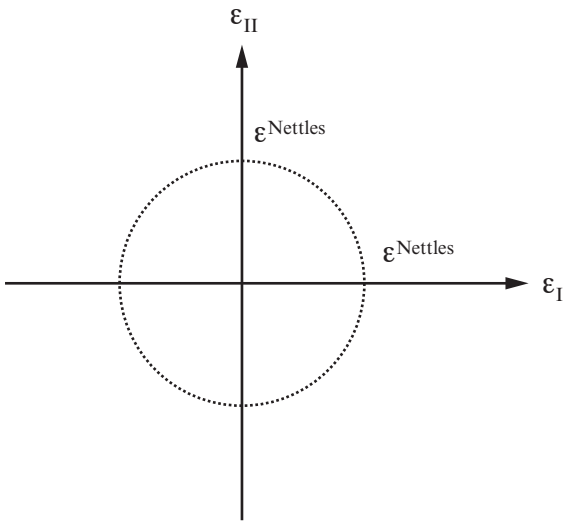

Figure 5. Graphical representation of the Nettles Circle failure criterion.

As it entails only one material performance parameter (a single strain limit, typically selected as the critical value from damage tolerant tension and compression load cases), Nettles Circle is straightforward to use and does not require traditional allowables development. The Nettles Circle approach is particularly applicable to damage tolerant design, as the strain limit can be developed/adjusted to account for damage in the material system of interest. In keeping with the authors' experience with damage tolerance in IM7/8552,[17,18,19] strain limits of 4,000 με (more conservative; based on compression) and 5,000 με (less conservative; based on tension) are considered in this study.

With each of the failure criteria considered herein, the strength ratio concept was utilized to aid in the thickness tailoring process. By considering a uniform factor R, by which each of the local stresses or strains are scaled, a failure criterion of interest can be used to characterize a given stress or strain state's proximity to the failure envelope. In this way, the strength ratio concept is of much more practical use than many traditional failure indices, which simply indicate 'failure' or 'no failure' in a qualitative manner without providing any quantitative insight as to how close (or

how far) a given stress or strain state is to the failure threshold. In its simplest form, the strength ratio concept is represented as:

$$\sigma_i^{max} = R\sigma_i^{applied}$$

or

$$\varepsilon_i^{max} = R\varepsilon_i^{applied} \tag{2}$$

where σ_i and ε_i are local stresses and local strains, respectively. A general representation of the strength-ratio concept is shown graphically (in 2D stress space) in Figure 6.

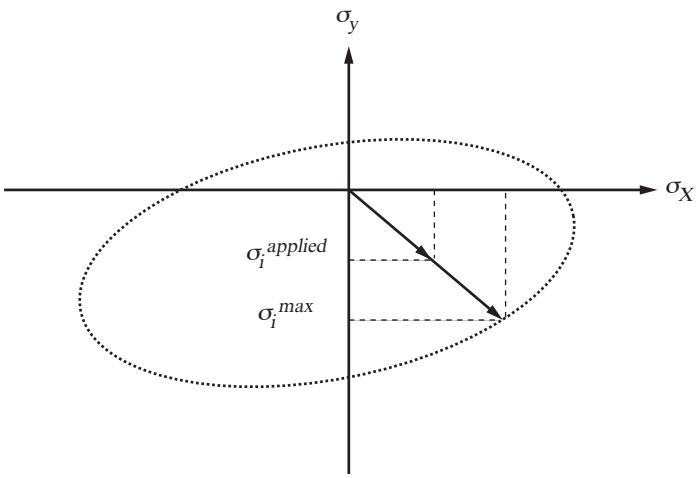

Figure 6. Graphical representation of the strength ratio concept in two-dimensional (2D) stress space. Note than an analog exists in 2D strain space.

Using the strength-ratio methodology, an *R* value of 1 entails a stress or strain state that is coincident with the failure envelope and therefore denotes failure. Further, an *R* value of 0.5 would denote failure where the applied stress or strain would need to be halved or the laminate thickness doubled to reach the failure envelope, while an *R* value of 2 would denote no failure where the applied stress or strain would need to be doubled or the laminate thickness halved to reach the failure envelope. Note that while *R* values less than 1 are useful in the aforementioned context of design, this situation is not physically possible (since failure is taken to occur at an *R* value of 1, additional stress or strain could not be applied beyond this point).

The determination of *R* values varies with failure theory given that the failure envelopes are different in shape/nature. For example, for Tsai-Wu, R is determined by solving the traditional Tsai-Wu failure criterion as a 2D-order polynomial, while for Nettles Circle, *R* is determined via a simple ratio of the strain limit to the critical principal strain. In solving for *R* values with various failure theories, care should be taken to ensure that results make physical sense, as disconnects

between mathematically valid solutions and physically significant solutions can arise in some cases. For example, where the solution to a 2D-order polynomial yields one positive root and one negative root, only the positive root should be taken. While both roots are mathematically valid in this case, only the positive root makes physical sense in light of how the strength ratio concept is defined.

While *R* values can be calculated 'manually' in post-processing, many commercially available FEA packages, including Abaqus, can provide output that enables the simple calculation of *R* values for commonly used failure criteria. By calling the CFAILURE field output for a composite layup in Abaqus, outputs for the Tsai-Wu, Tsai-Hill, and Maximum Stress failure criteria were retrieved in this study. *R* values for each of these failure criteria were then calculated by taking the inverse of the respective Abaqus output values. For the sake of clarity, equation (3) shows the calculation of *R* values for the Tsai-Wu failure criterion.

$$R_{Tsai\text{-}Wu} = \frac{1}{TSAIW} \tag{3}$$

For Nettles Circle, critical principal strains were used along the selected strain limits to calculate corresponding *R* values. In each case (regardless of the failure criterion considered), critical *R* values were determined for seven layup regions within the composite sandwich acreage in the adapter. These seven layup regions are shown in Figure 7.

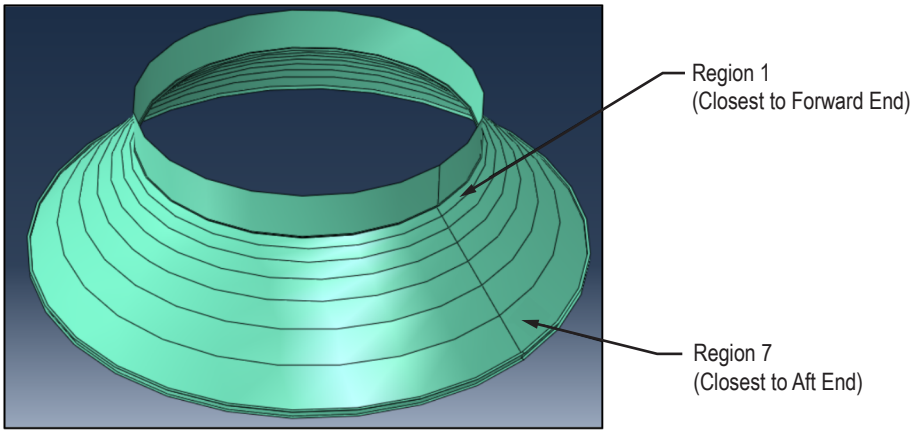

Figure 7. Layup regions considered for thickness tailoring in the adapter's composite sandwich acreage.

Note that layup regions are smaller in width toward the forward end of the adapter. Given the structure's frustum geometry, line load into the composite sandwich acreage is larger in magnitude at the smaller-diameter forward end than at the larger-diameter aft end. As such, layup regions were laid out smaller in width toward the forward end to allow for additional fidelity in thickness tailoring. To facilitate rapid iterations in the strength optimization process, a Python™ script was used to process critical *R* values for each of the failure theories considered herein.

2.4 Linear Buckling Analysis

To address structural stability in the adapter, simple linear buckling analyses (no geometric imperfections or nonlinear structural behavior considered) were carried out. Eigenvalues, denoted as $\lambda_{buckling}$, associated with the first valid buckling mode were taken. Though linear buckling solvers commonly available in FEA packages (including Abaqus) are considered to be accurate, care was taken to ensure that predicted buckling modes were realistic and applicable in the context of the adapter. While more detailed buckling analyses may ultimately be considered further into a typical design/analysis cycle, the linear buckling analyses considered in the case study presented herein are commonly used for preliminary sizing and provide for rapid iteration in the interest of design optimization (given this practical convenience, linear buckling analyses may be relied upon to some extent even beyond preliminary sizing).

2.5 Natural Frequency Analysis

Given that launch vehicle structures are commonly subject to significant vibration and acoustic loads, straightforward analyses were carried out to determine the natural frequency for each structural configuration considered herein. In particular, natural frequencies were extracted for the first natural frequency mode using Abaqus' built-in Lanczos eigensolver. A 75-t mass was placed at the same reference point used for load introduction in the strength and buckling analyses (refer to Figure 4 for detail) 60 in above the forward end of the load introduction structure and centered within the load introduction structure/adapter. No additional loads were applied (i.e., no P_{eq} or 'crush' pressure on the composite sandwich acreage) in the natural frequency analyses in the interest of conservatism, since the addition of compressive loads in this case serves to increase the adapter's apparent natural frequency. The same boundary conditions at the aft end used for strength and buckling analyses were also used for natural frequency analyses.

Given the intentionally generic nature of this case study, a target natural frequency, as would be commensurate with a particular flight application's structural dynamics requirements, was not considered. Considering this, natural frequency values are simply reported (in the interest of completeness) for each of the configurations considered herein for the adapter.

2.6 Safety Factors, Knockdown Factors, and Margins of Safety

For strength and buckling analyses, typical safety factors consistent with NASA technical standards were considered. Per NASA-STD-5001B,[20] a safety factor of 1.4 (minimum design factor for composite structures where the prototype verification approach is used) was considered for both strength and buckling analyses in the composite sandwich acreage.

Given that the adapter considered in this study was assumed to be geometrically perfect, a buckling knockdown factor (KDF) was used to account for differences between the as-modeled structure and what would be expected in the as-built structure. In the interest of generating a conservative design, especially in the preliminary sizing process, a buckling KDF is commonly used for thin-walled shell structures considering that geometric imperfections in an as-built structure (which can be reasonably expected) can lead to buckling loads much lower than the theoretical buckling load calculated for a geometrically perfect structure.[21] While the general

need for a buckling KDF is clear, the selection of a particular value for the adapter considered herein is not straightforward. The most widely considered NASA guidance on buckling KDFs for thin-walled shell structures[22,23] was last updated in the late 1960s and did not directly consider composite shell structures. In particular, NASA SP-8019 recommends a universal buckling KDF of 0.33 (that is, the buckling load in an as-built structure is taken as 33% of the theoretical buckling load) for conical shells.[23] However, this 1960s-era guidance is widely considered to be overly conservative and has thus drawn interest within NASA and across the aerospace industry as a whole. Most notably, the NASA Engineering and Safety Center (NESC) has pursued an experimental- and analytical-based approach via the shell buckling knockdown factor (SBKF) project in an effort to revise NASA's guidance on buckling KDFs in thin-walled cylindrical shells (both metallic and composite). Perhaps most applicable to this case study, Sleight, et al.[21] evaluated buckling imperfection sensitivity in conical sandwich composite structures with characteristics similar to the adapter considered herein. They modeled geometric imperfections in conical shell structures based on as-measured imperfection data gathered for a cylindrical sandwich composite structure that was built and tested as part of the SBKF project. Upon considering a wide range of imperfection profiles, Sleight, et al. showed that normalized buckling load (nonlinear buckling load considering geometric imperfections divided by theoretical linear buckling load considering no geometric imperfections) was higher than 0.5 in all cases and was higher than 0.6 in all but two cases. While further study (including an experimental component) can help to further substantiate this data, these findings suggest that there is significant conservatism in the currently recommended buckling KDF of 0.33. As such, in keeping with the findings reported by Sleight, et al.[21], a buckling KDF of 0.5 is used in this case study. Safety and KDFs considered in this study are summarized in Table 4.

Table 4. Safety and KDFs considered in adapter case study.

Category	Applicability	Value
Safety factor	Strength (composite sandwich acreage)	1.4
Safety factor	Buckling (composite sandwich acreage)	1.4
Knockdown factor	Buckling (composite sandwich acreage)	0.50

Using these safety factors and KDFs, margins of safety were calculated per equations (4) and (5):

$$MS_{strength} = \frac{R}{SF_{strength}} - 1 \tag{4}$$

$$MS_{buckling} = \frac{\lambda_{buckling} * KDF_{buckling}}{SF_{buckling}} - 1 \tag{5}$$

where,

MS = margin of safety
SF = safety factor
R = strength ratio as defined in equation (2)
$\lambda_{buckling}$ = eigenvalue associated with the first buckling mode.

3. RESULTS AND DISCUSSION

3.1 Adapter Configurations Using Quasi-isotropic Layups

To facilitate meaningful comparisons in this study, adapter configurations were first established using quasi-isotropic facesheet layups. In particular, a [+45/0/–45/90] layup family was selected. Considering the loads detailed in section 2.2, a P_{eq} of 1,356,814 lbf and a uniform 'crush' pressure (on the composite sandwich acreage only) of 0.1 psi, R values and associated margins of safety were calculated for the Tsai-Wu, Tsai-Hill, Maximum Stress, and Nettles Circle (with 5,000 με and 4,000 με) failure theories. Given that the load case considered herein is compression dominant, the more conservative Nettles Circle strain limit of 4,000 με is preferred given that it is based on compression performance. Thus, the results corresponding to a Nettles Circle strain limit of 5,000 με are included for comparison purposes only. Eigenvalues for the first valid buckling mode, associated margins of safety, and natural frequencies were also determined.

As seen in Table 5, Nettles Circle with a strain limit of 4,000 με is the failure criterion that yields the smallest margins of safety (which is to be expected, as it is the most conservative failure criterion used herein). As expected with the adapter's frustum geometry, the forward end is the critical region with respect to strength. The 16-ply [+45/0/–45/90] configuration, that is, the 'baseline' configuration where the facesheets are 16 plies throughout the entire adapter, showed large enough strength margins near the aft end to warrant further evaluation of facesheet thickness in this region. As mentioned in section 1.2, effective repeating unit size for a [+45/0/–45/90] layup is 8 plies (where layup composition, balance, and symmetry are maintained). Despite the low level of fidelity associated with an 8-ply effective repeating unit in a 16-ply layup, the quasi-isotropic adapter configuration was able to be tailored in regions 6 and 7 (the two regions nearest the aft end). The optimized [+45/0/–45/90] configuration provides for 22% weight savings over the baseline 16-ply configuration. Note that contour plots for the quasi-isotropic configurations are presented in Figures 9 and 10 in appendix A.

Table 5. Results for adapter using [+45/0/–45/90]s layup. Values in italics represent margins of safety.

			R Values (first ply failure, where applicable)							
	Layup Region	Ply Count	Tsai-Wu	Tsai-Hill	Max Stress	Nettles Circle (5,000 με)	Nettles Circle (4,000 με)	Eigenvalue, First Buckling Mode	Natural Frequency (Hz)	Estimated Weight (Shell Only)
Baseline [+45/0/-45/90]	1	16	5.25 *(+2.75)*	3.58 *(+1.56)*	3.67 *(+1.62)*	1.86 *(+0.33)*	1.48 *(+0.06)*	4.84 *(+0.73)*	5.93	1,007 lb
	2	16	12.1 *(+7.64)*	5.93 *(+3.23)*	6.14 *(+3.38)*	3.12 *(+1.23)*	2.50 *(+0.78)*			
	3	16	6.35 *(+3.54)*	4.66 *(+2.33)*	5.12 *(+2.66)*	2.79 *(+0.99)*	2.23 *(+0.59)*			
	4	16	5.61 *(+3.00)*	4.43 *(+2.16)*	4.69 *(+2.35)*	2.78 *(+0.99)*	2.23 *(+0.59)*			
	5	16	5.66 *(+3.04)*	4.59 *(+2.28)*	4.79 *(+2.42)*	3.10 *(+1.21)*	2.48 *(+0.77)*			
	6	16	6.27 *(+3.48)*	5.24 *(+2.74)*	5.41 *(+2.86)*	3.68 *(+1.63)*	2.94 *(+1.10)*			
	7	16	6.56 *(+3.69)*	5.43 *(+2.88)*	5.63 *(+3.02)*	3.52 *(+1.52)*	2.82 *(+1.01)*			
Optimized [+45/0/-45/90]	1	16	5.29 *(+2.78)*	3.58 *(+1.56)*	3.67 *(+1.62)*	1.86 *(+0.33)*	1.48 *(+0.06)*	3.17 *(+0.13)*	5.59	783 lb (–22%)
	2	16	12.4 *(+7.82)*	5.91 *(+3.22)*	6.12 *(+3.37)*	3.11 *(+1.22)*	2.49 *(+0.78)*			
	3	16	6.53 *(+3.66)*	4.77 *(+2.41)*	5.25 *(+2.75)*	2.84 *(+1.03)*	2.28 *(+0.68)*			
	4	16	5.65 *(+3.03)*	4.55 *(+2.25)*	4.79 *(+2.42)*	2.85 *(+1.04)*	2.28 *(+0.63)*			
	5	16	5.32 *(+2.80)*	4.65 *(+2.32)*	4.74 *(+2.39)*	3.23 *(+1.30)*	2.58 *(+0.84)*			
	6	8	3.49 *(+1.49)*	2.83 *(+1.02)*	2.95 *(+1.11)*	1.91 *(+0.37)*	1.53 *(+0.09)*			
	7	8	3.55 *(+1.54)*	2.87 *(+1.05)*	3.00 *(+1.14)*	1.92 *(+0.37)*	1.54 *(+0.10)*			

3.2 Optimized Configuration using [±θ] Layup

Following the evaluation of the quasi-isotropic adapter configurations, the [±θ] layup configurations were evaluated. To select the optimal ply angle θ, the adapter (with 16-ply facesheets) was evaluated for strength, linear buckling, and natural frequency across a range of values from $\theta = 0°$ to $\theta = 45°$ in 5° increments. Model parameters, including material properties, geometries, boundary conditions, and applied loads, were held constant between the quasi-isotropic and [±θ] layup configurations. Facesheet layup definition was altered via the composite layup editor in Abaqus. Results of this survey are shown in Figure 8. Note that *R* values, buckling eigenvalues, and natural frequency values are normalized by the corresponding values for the previously evaluated 16-ply [+45/0/–45/90] layup configuration.

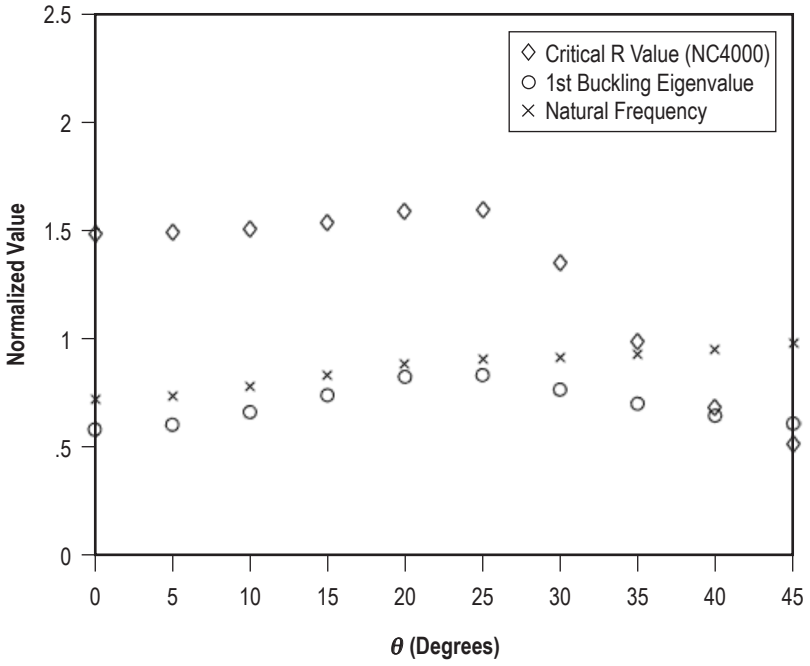

Figure 8. Survey of adapter performance using 16-ply [±θ] layups. Note that a normalized value of 1 for a given performance characteristic (strength, buckling, or natural frequency) corresponds to that of an adapter using a 16-ply [+45/0/–45/90] layup.

Considering the results shown in Figure 8, a [±θ] layup where $\theta = 25°$, the best performer among [±θ] layups with respect to strength and linear buckling, was selected. In the interest of comparison, an adapter configuration was first evaluated with 16-ply [±25] facesheets. As expected, based on the results shown in figure 8, the 16-ply [±25] adapter configuration showed higher strength margins and lower buckling margins compared to the 16-ply [+45/0/–45/90] adapter configuration. Taking advantage of the 4-ply effective repeating unit in the [±25] facesheets, the adapter was tailored. As was the case with the quasi-isotropic configurations, Nettles Circle with a strain limit of 4,000 με is the critical failure criterion with the [±25] configurations. Unlike the quasi-isotropic configurations where strength controlled (critical strength margin of safety was lower than buckling margin of safety), linear buckling controlled in the [±25] configurations (buckling margin of safety was lower than critical strength margin of safety), as seen in table 6. Through a series of iterations (the *R* value approach is of limited use where strength is not critical), the optimized [±25] configuration shown in the bottom half of Table 6 was selected. The optimized [±25] configuration provides for 27% weight savings over the baseline 16-ply configuration. These weight savings compare favorably to the 22% weight savings possible using quasi-isotropic facesheets, though the value of an additional 5% in weight savings may vary depending on the application at hand.

Table 6. Optimization results for conical shell using [+25/–25] layup family. Values in italics represent margins of safety.

			R Values (first ply failure, where applicable)							
	Layup Region	Ply Count	Tsai-Wu	Tsai-Hill	Max Stress	Nettles Circle (5,000 με)	Nettles Circle (4,000 με)	Eigenvalue, First Buckling Mode	Natural Frequency (Hz)	Estimated Weight (Shell Only)
Baseline [±25]	1	16	7.65 *(+4.47)*	5.35 *(+2.82)*	5.74 *(+3.10)*	2.93 *(+1.10)*	2.35 *(+0.68)*	4.00 *(+0.43)*	5.35	1,007 lb
	2	16	14.1 *(+9.10)*	7.24 *(+4.17)*	7.83 *(+4.60)*	3.79 *(+1.71)*	3.03 *(+1.16)*			
	3	16	11.3 *(+7.04)*	9.06 *(+5.47)*	11.5 *(+7.19)*	5.37 *(+2.84)*	4.30 *(+2.07)*			
	4	16	4.57 *(+2.27)*	5.25 *(+2.75)*	6.10 *(+3.36)*	4.07 *(+1.91)*	3.25 *(+1.32)*			
	5	16	3.42 *(+1.44)*	4.06 *(+1.90)*	4.91 *(+2.51)*	3.64 *(+1.60)*	2.91 *(+1.08)*			
	6	16	3.39 *(+1.42)*	4.02 *(+1.87)*	4.89 *(+2.49)*	3.59 *(+1.56)*	2.87 *(+1.05)*			
	7	16	4.35 *(+2.11)*	5.13 *(+2.66)*	6.08 *(+3.34)*	4.47 *(+2.19)*	3.58 *(+1.55)*			
Optimized [±25]	1	12	7.54 *(+4.38)*	4.16 *(+1.97)*	4.46 *(+2.19)*	2.18 *(+0.55)*	1.74 *(+0.24)*	2.83 *(+0.01)*	5.18	731 lb (–27%)
	2	12	13.0 *(+8.31)*	5.63 *(+3.02)*	6.01 *(+3.30)*	2.98 *(+1.13)*	2.38 *(+0.70)*			
	3	12	7.25 *(+4.18)*	6.43 *(+3.59)*	8.24 *(+4.89)*	3.98 *(+1.84)*	3.18 *(+1.27)*			
	4	12	3.37 *(+1.40)*	3.90 *(+1.78)*	4.54 *(+2.24)*	3.10 *(+1.21)*	2.48 *(+0.77)*			
	5	12	2.61 *(+0.86)*	3.09 *(+1.21)*	3.76 *(+1.68)*	2.76 *(+0.97)*	2.21 *(+0.58)*			
	6	12	2.59 *(+0.85)*	3.08 *(+1.20)*	3.76 *(+1.68)*	2.73 *(+0.95)*	2.18 *(+0.56)*			
	7	8	2.98 *(+1.13)*	3.37 *(+1.41)*	3.91 *(+1.79)*	2.53 *(+0.80)*	2.02 *(+0.44)*			

As previously mentioned, Nettles Circle with a 4,000 με strain limit was the critical failure theory among those considered in this study. This is to be expected, given that the Nettles Circle cutoff strain is a lower bound value preset to account for damage tolerance and environmental effects. Note that this is in contrast to the ply-by-ply failure analyses, which do not account for damage tolerance or environmental effects and therefore do not provide a complete evaluation in this way. Furthermore, the widely varying *R* value magnitudes and associated trends among the ply-by-ply failure theories considered gives further credence to the idea that ply-by-ply failure theories should be used only where the tendencies and sensitivities are comprehensively understood in the context of the materials and structural application(s) of interest.

It is recognized that the specific trends and characteristics associated with the results presented in Tables 5 and 6 are likely to vary with structural configuration (materials, geometry, boundary conditions, applied loads, etc.). However, it is reasonable to consider that weight savings opportunities offered by optimized [±θ] layups may be more pronounced in strength-critical applications where the full extent of their considerable tailorability can be fully utilized.

3.3 Implications with Respect to Testing and Design Substantiation

Given that the effective repeating unit concept (discussed in detail in sections 1.1 and 1.2) was utilized in the thickness tailoring process, each of the optimized configurations presented in tables 5 and 6 entails only one composite layup family to be qualified. This is the case since layup composition, balance, and symmetry are maintained through the thickness tailoring process such that a single set of laminate-level properties is applicable throughout the structure even as laminate thickness varies in the interest of optimization. Note that this applies to both the [+45/0/–45/90] and [±25] adapter configurations. That is, if the effective repeating unit concept (as defined herein) is utilized, thickness tailoring can be carried out such that the number of layup families to be qualified can be minimized. This can help to minimize the scope of testing needed to substantiate a given design, which is of obvious significance with respect to both schedule and cost. It should be noted, however, that optimization via thickness tailoring may bring on additional design complexity at/near transition regions (i.e., where plies are added/dropped). The need to characterize these transition regions may offset, at least to some degree, the reduction in testing scope associated with minimizing the number of layup families to be qualified. The trade between these two potentially competing interests is likely to vary with structural configuration, and as such, should be carefully assessed for the application of interest.

The scope of testing needed to substantiate a given design may be further minimized if the Nettles Circle failure criterion is utilized. Given that a governing strain limit is used regardless of layup family, laminate-level properties are not explicitly required to write margins of safety. Though testing may be required to verify the Nettles Circle strain limit for a given layup family, this testing is likely to be far more limited in scope compared to that required for traditional laminate-level strength allowables.

While the effective repeating unit concept can be useful in practice for any number of layup families, minimizing the size of the effective repeating unit maximizes the potential for laminate thickness tailoring as initially discussed in section 1.1. As evidenced in tables 5 and 6, [±θ] layups offer additional opportunities for thickness tailoring due to their minimal effective repeating unit size. This, in turn, provides for flexibility over the course of a project given that design changes can be readily addressed all the while minimizing weight in the structure. Coupled with the aforementioned potential for reduced testing scope where the effective repeating unit concept is used, [±θ] layups can provide for design flexibility without significant schedule and/or cost impacts.

4. CONCLUDING REMARKS

This study demonstrates an approach to better realize the benefits of tailoring in composite structures through the use of [±θ] layups. In particular, an adapter (with conventional composite sandwich acreage) typical of a large-scale launch vehicle is considered. A case study is carried out to evaluate the potential of the [±θ] layup concept with respect to tailorability via laminate thickness optimization. Through strength, buckling, and natural frequency analyses, the adapter considered herein is tailored using a [±25] layup family in the composite sandwich facesheets. Results show that weight savings of 5% can be achieved using this [±θ] layup family compared to a traditional quasi-isotropic layup, all the while maintaining a single layup family for the purposes of design substantiation.

In view of this case study and the accompanying discussion, the following remarks should be considered with respect to the use of [±θ] layups and the Nettles Circle failure criterion in composite structures:

- Real-world constraints typical of large-scale composite structure projects/programs, including cost, schedule, and risk, often dictate that the number of composite layups to be qualified should be minimized.
- [±θ] layups provide for improved thickness tailoring due to minimal effective repeating unit size, thus providing for tailorability where a minimal number of composite layups must be qualified. In this way, [±θ] layups may offer a practical route to optimization in composite structures (typically difficult to realistically achieve), thereby allowing enhanced weight savings and/or performance characteristics to be more fully realized.
- If the Nettles Circle failure criterion is used (where a preset damage tolerant strain limit is utilized), traditional laminate-level strength allowables may not be required to substantiate a given design.
- While thickness tailoring can entail additional design complexity at/near transition regions, [±θ] layups may provide for significant design flexibility even through the late stages of a project. This additional design flexibility can be especially critical where evolving design requirements must be accommodated within the constraints of a typical large-scale composite structure project/program.
- The flexibility afforded by the minimal effective repeating unit size in [±θ] layups, which may allow a composite structure to be readily adapted in light of design changes over the course of a project while minimizing weight and avoiding significant schedule and/or cost impacts, is seen by the authors to be the most significant practical benefit.

APPENDIX A—CONTOUR PLOTS FROM ADAPTER OPTIMIZATION RUNS

Contour plots for each of the adapter configurations considered in this study are shown in this appendix (Figures 9–12). Note that in these figures, only the composite sandwich acreage (adapter shell structure) is shown for clarity. Furthermore, for Figures 10 and 12, in linear buckling analyses in Abaqus, mode shapes do not represent actual magnitudes of deformation at critical buckling load (displacements are normalized so that the maximum individual displacement component is 1).

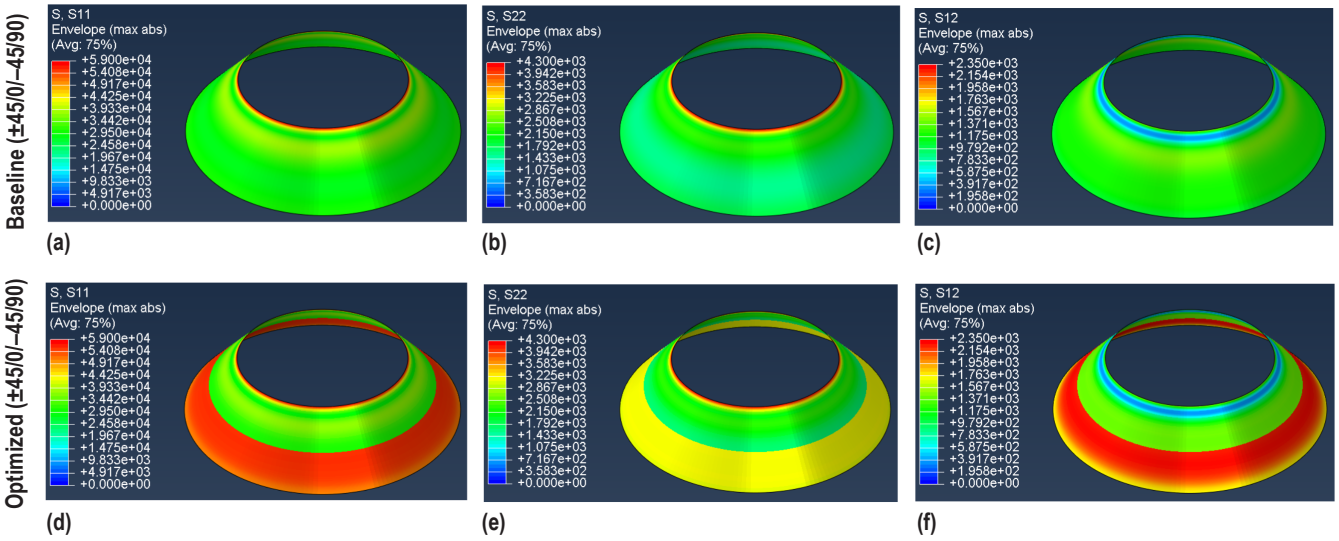

Figure 9. Local stresses (units: psi) for adapter using [+45/0/–45/90] layup family. For baseline [+45/0/–45/90] configuration: (a) S11, (b) S22, and (c) S12. For optimized [+45/0/–45/90] configuration: (d) S11, (e) S22, and (f) S12.

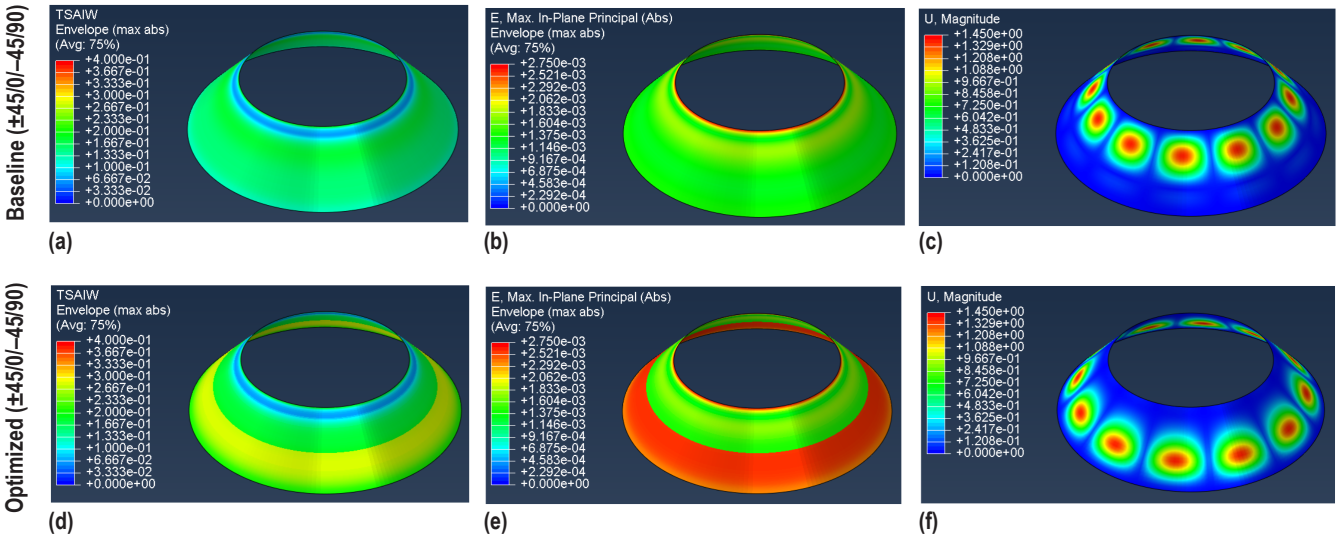

Figure 10. Contour plots for adapter using [+45/0/–45/90] layup family. For baseline [+45/0/–45/90] configuration: (a) Tsai-Wu (unitless), (b) maximum in-plane principal strain (units: in/in), and (c) magnitude of total deformation associated with first buckling mode (units: in). For optimized [+45/0/–45/90] configuration: (d) Tsai-Wu, (e) maximum in-plane principal strain, and (f) magnitude of total deformation associated with first buckling mode.

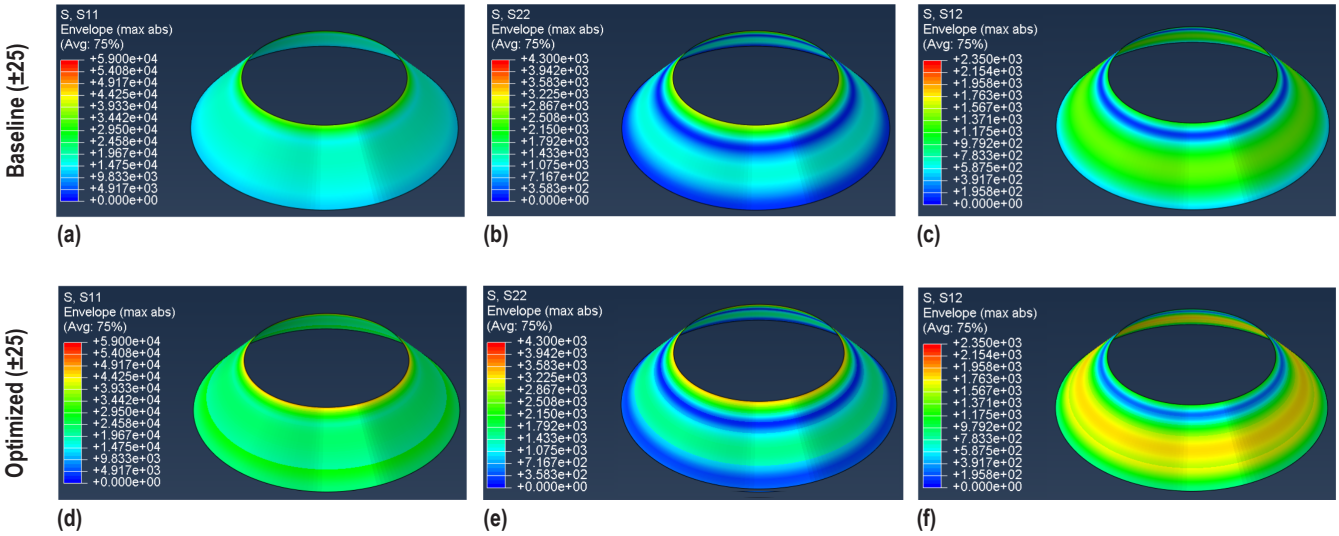

Figure 11. Local stresses (units: psi) for adapter using [±25] layup family. For baseline [±25] configuration: (a) S11, (b) S22, and (c) S12. For optimized [±25] configuration: (d) S11, (e) S22, and (f) S12.

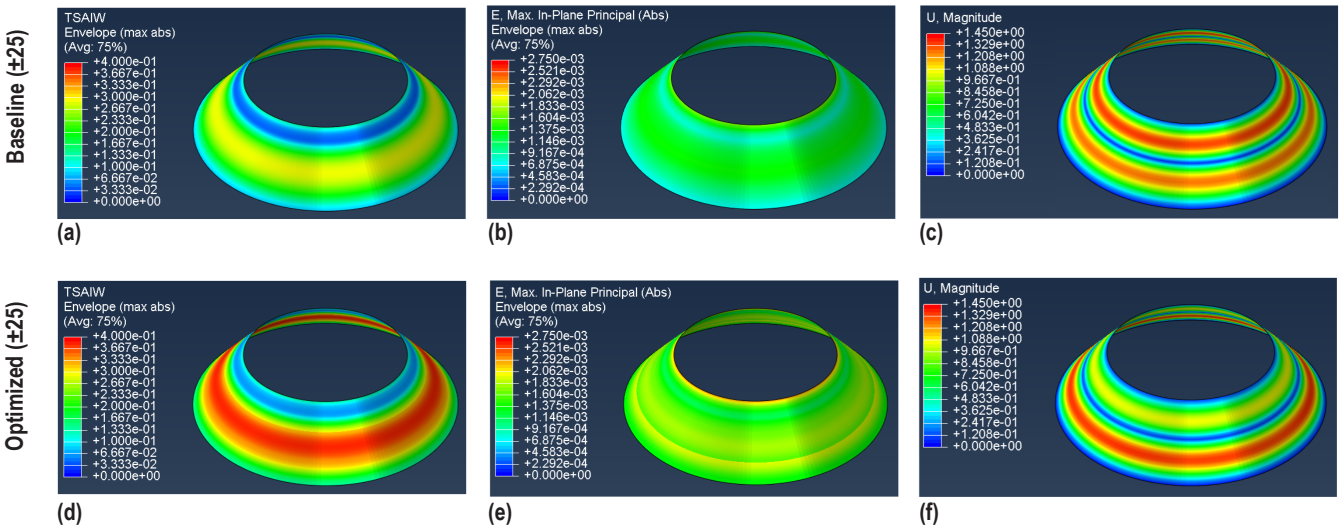

Figure 12. FEA contour plots for adapter using [±25] layup family. For baseline [±25] configuration: (a) Tsai-Wu (unitless), (b) maximum in-plane principal strain (units: in/in), and (c) magnitude of total deformation associated with first buckling mode (units: in). For optimized [±25] configuration: (d) Tsai-Wu, (e) maximum in-plane principal strain, and (f) magnitude of total deformation associated with first buckling mode.

APPENDIX B—DERIVATION OF EQUIVALENT AXIAL LOAD FOR AXISYMMETRIC STRUCTURE

Consider a thin shell axisymmetric structure with an applied axial load P and overturning moment M, such as the conical frustum shell shown in Figure 13.

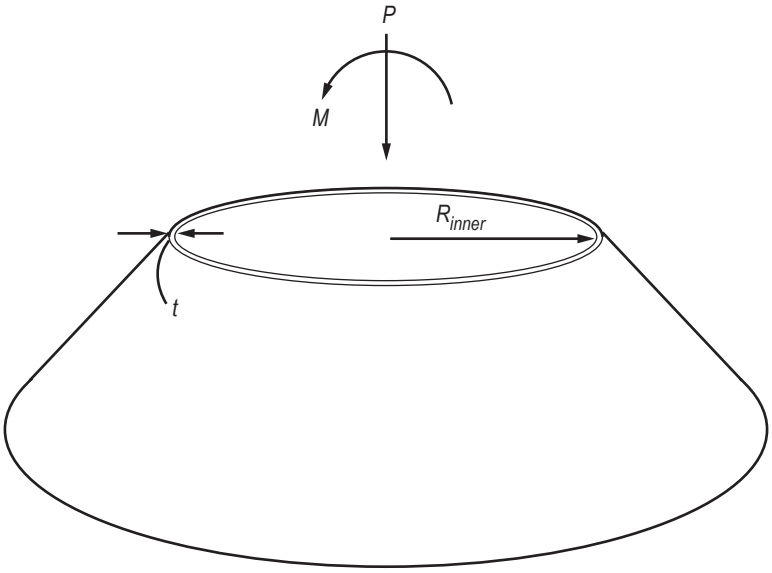

Figure 13. Thin shell conical frustum with applied axial load *P* and overturning moment *M*.

where shell thickness is defined by t and is considerably smaller than the radius of the axisymmetric structure (threshold for 'thin' is commonly taken as $t/R_{nominal} < 0.1$). Note that the outer radius is defined by

$$R_{outer} = R_{inner} + t \tag{6}$$

A nominal radius, formally defined as the average of the inner and outer radii, can be written as:

$$R_{nominal} = \frac{R_{inner} + R_{outer}}{2} \tag{7}$$

In order to develop an expression for an equivalent axial load P_{eq} (see section 2.3 for further context and discussion), the applied axial load and overturning moment can first be written as equivalent line loads at the forward end of the axisymmetric structure. Then, these combined equivalent line loads can be 'converted' to an equivalent axial load by taking the nominal circumference of the forward end into consideration.

For the applied axial load P, the equivalent line load at the forward end N_p can be written as

$$N_P = \sigma_P t = \frac{P}{A} t \tag{8}$$

where A is the cross-sectional area at the forward end and is precisely defined as

$$A = \pi \left(R_{outer}^2 - R_{inner}^2 \right) \tag{9}$$

However, given the thin shell condition, the cross-sectional area at the forward end can be approximated as the nominal circumference multiplied by shell thickness.

$$A = 2\pi R_{nominal} t \tag{10}$$

Using this approximation, equation (8) can be rewritten for the equivalent line load at the forward end:

$$N_P = \frac{P}{2\pi R_{nominal} t} t = \frac{P}{2\pi R_{nominal}} \tag{11}$$

For the applied overturning moment M, the equivalent line load at the forward end can be written in a similar manner

$$N_M = \pm \sigma_M t = \pm \frac{Mc}{I} t \tag{12}$$

where,

c = perpendicular distance from the thin shell at the forward end to the central axis of the axisymmetric structure

I = area moment of inertia (second moment of area) of the thin shell at the forward end about the central axis of the axisymmetric structure.

Given the thin shell condition, the perpendicular distance can be approximated as the nominal radius at the forward end $R_{nominal}$. Then, equation (12) can be written as

$$N_M = \pm \frac{M R_{nominal}}{\frac{\pi}{4} \left(R_{outer}^4 - R_{inner}^4 \right)} t \tag{13}$$

Substituting equation (6) into equation (13) and expanding the fourth order polynomial yields

$$\begin{aligned} N_M &= \pm \frac{4 M R_{nominal}}{\pi \left[(R_{inner} + t)^4 - R_{inner}^4 \right]} t \\ &= \pm \frac{4 M R_{nominal}}{\pi \left[(R_{inner}^4 + 4 R_{inner}^3 t + 6 R_{inner}^2 t^2 + 4 R_{inner} t^3 + t^4) - R_{inner}^4 \right]} t \end{aligned} \tag{14}$$

Given the thin shell condition, higher order terms involving shell thickness can reasonably be neglected (t^2, t^3, $t^4 \approx 0$). This allows for simplification of equation (14).

$$N_M = \pm \frac{4MR_{nominal}}{\pi\left[(R_{inner}^4 + 4R_{inner}^3 t)\text{-}R_{inner}^4\right]} t = \pm \frac{4MR_{nominal}}{\pi(4R_{inner}^3 t)} \mathrm{t} = \pm \frac{MR_{nominal}}{\pi R_{inner}^3} \tag{15}$$

Again, considering the thin shell condition, the $R^3{}_{inner}$ term can be approximated as $R^3{}_{nominal}$. This allows for further simplification of equation (15).

$$N_M = \pm \frac{M}{\pi R_{nominal}^2} \tag{16}$$

Taking equations (11) and (16), the combined maximum equivalent line load for the applied axial load P and overturning moment M can then be written as

$$N_{eq} = N_P \pm N_M = \frac{P}{2\pi R_{nominal}} \pm \frac{M}{\pi R_{nominal}^2} \tag{17}$$

Considering the nominal circumference of the axisymmetric structure at the forward end, $2\pi R_{nominal}$, the equivalent line load N_{eq} can be 'converted' to an equivalent axial load P_{eq} written as

$$P_{eq} = N_{eq}(2\pi R_{nominal}) = P \pm \frac{2M}{R_{nominal}} \tag{18}$$

REFERENCES

1. Guin, W.E.; Phillips, D.R.: "Examining the Relationship between Basis Values and Ply-by-ply Failure Theories for Composite Structures," in *AIAA Scitech 2019 Forum*, January 7–11, 2019, San Diego, CA, doi:10.2514/6.2019-0519.

2. Tsai, S. W.; Melo, J.D.D; Sihn, S.; et al.: *Composite Laminates: Theory and practice of analysis, design and automated layup*, Stanford Aeronautics and Astronautics, Springer International Publishing, Basel, Switzerland, pp. 241–282, March 2017.

3. Tsai, S.W.; Guin, W.E.; Riccio, A.; et al.: "Weight and Cost Reduction with Double-Double Laminates," *JEC Composites Magazine*, Vol. 135, pp. 64–65, November 2020.

4. Clarkson, E.: "Hexcel 8552 IM7 Unidirectional Prepreg 190 gsm and 35%RC Qualification Statistical Analysis Report," NCAMP Test Report CAM-RP-2009-015 Rev A, Wichita State University, Wichita, KS, April 22, 2011.

5. *Composite Materials Handbook-17 (CMH-17)*, Revision G, SAE International, July 2012.

6. Flaggs, D.L.; Kural, M.H.: "Experimental Determination of the In Situ Transverse Lamina Strength in Graphite/Epoxy Laminates," *Journal of Composite Materials*, Vol. 16, pp. 103–116. doi:10.1177/002199838201600203, March 1, 1982.

7. "Hexcel Product Data Sheet for HexWeb CR III Corrosion Resistant Specification Grade Aluminum Honeycomb," Hexcel Corporation, 2017.

8. Gibson, L.J.; Ashby, M.F.: *Cellular Solids: Structure and Properties*, Cambridge University Press, Cambridge, UK, August 1999.

9. King, W.T.; Guin, W.E.; Jordon, J.B.; et al.: "Effects of Honeycomb Core Damage on the Performance of Composite Sandwich Structures," *Journal of Composite Materials*, Vol. 54, pp. 2,159–2,171, doi:10.1177/0021998319890656, December 2019.

10. Bugg, F.; Brunty, J.; Ernsberger, G.: et al.: "National Launch System Cycle I Loads and Mod els Data Book," NASA/TM—1992—103560, NASA Marshall Space Flight Center, Huntsville, AL, 1992.

11. Macheske, V.; Womack, J.; and Binkley, J.: "A Statistical Technique for Combining Launch Vehicle Atmospheric Flight Loads," in: Proc. 31st Aerospace Sciences Meeting, Reno, NV, doi:10.2514/6.1993-755, January 11–14, 1993.

12. Ford, D.B.: "Equivalent Maximum Line Load From Applied Axial Forces, Bending Moments, and Pressures," Technical Report TCD-99-004, 2009.

13. Hinton, M.J.; Kaddour, A.S.; and Soden, P.D. (eds.): *Failure Criteria in Fibre-Reinforced-Polymer Composites: The World-Wide Failure Exercise*, Elsevier Science, Science Direct, 2004.

14. Hinton, M.J.; and Soden, P.D.: "Predicting Failure in Composite Laminates: The Background to The Exercise," *Composites Science and Technology*, Vol. 58, No. 7, pp. 1001–1010, doi:10.1016/S0266-3538(98)00074-8, July 1998.

15. Tsai, S.W.; and Melo, J.D.D: "A Unit Circle Failure Criterion for Carbon Fiber Reinforced Polymer Composites," *Composites Science and Technology*, Vol. 123, pp. 71–78, doi:10.1016/j.compscitech.2015.12.011, 2016.

16. Melo, J.D.D; Bi, J.; and Tsai, S.W.: "A Novel Invariant-Based Design Approach to Carbon Fiber Reinforced Laminates," *Composite Structures*, Vol. 159, pp. 44–52, doi:10.1016/j.compstruct.2016.09.055, September 2016.

17. Nettles, A.T.; Jackson, J.R.; and Guin, W.E.: "Sandwich Structure Risk Reduction in Support of the Payload Adapter Fitting," NASA/TM-2018-219849, NASA Marshall Space Flight Center, Huntsville, Alabama, 2018.

18. Nettles, A.T.; Guin, W.E.; Jackson, J.R., and Cox, S.B.: "Repair of Sandwich Structure in Support of the Payload Adapter Fitting," NASA/TM-2018-219866, NASA Marshall Space Flight Center, Huntsville, Alabama, 2018.

19. Nettles, A.T.; Guin, W.E.; Jackson, J.R., and Mavo, J.P.: "Repair of Sandwich Structure in Support of the Payload Adapter Fitting Part II: Severe Damage Repair," NASA/TM-2020-220556, NASA Marshall Space Flight Center, Huntsville, Alabama, 2020.

20. NASA-STD-5001B, "Structural Design Requirements and Factors of Safety for Spaceflight Hardware," NASA, Washington, D.C., 2016.

21. Sleight, D.W.; Satyanarayana, A.; Li, Y.; and Schultz, M.R.: "Buckling Imperfection Sensitivity of Conical Sandwich Composite Structures for Launch-Vehicles," in *AIAA/ASCE/AHS/ASC Structures, Structural Dynamics, and Materials Conference*, January 8–12, 2018, Aerospace Research Central, Kissimmee, Florida, pp. 1–17, doi:10.2514/6.2018-1696, 2018.

22. NASA SP-8007, "Buckling of Thin-Walled Circular Cylinders," NASA Langley Research Center, Hampton, Virginia, 1968.

23. NASA SP-8019, "Buckling of Thin-Walled Truncated Cones," NASA Marshall Space Flight Center, Huntsville, Alabama, September 1968.

REPORT DOCUMENTATION PAGE

Form Approved
OMB No. 0704-0188

1. REPORT DATE *(DD-MM-YYYY)*	2. REPORT TYPE	3. DATES COVERED *(From - To)*
01–11–2021	Technical Memorandum	

4. TITLE AND SUBTITLE

A Straightforward Approach to Thickness Tailoring in Composite Structures Using Non-traditional Layups

5a. CONTRACT NUMBER

5b. GRANT NUMBER

5c. PROGRAM ELEMENT NUMBER

6. AUTHOR(S)

W.E. Guin and A.T Nettles

5d. PROJECT NUMBER

5e. TASK NUMBER

5f. WORK UNIT NUMBER

7. PERFORMING ORGANIZATION NAME(S) AND ADDRESS(ES)

George C. Marshall Space Flight Center
Huntsville, AL 35812

8. PERFORMING ORGANIZATION REPORT NUMBER

M–1534

9. SPONSORING/MONITORING AGENCY NAME(S) AND ADDRESS(ES)

National Aeronautics and Space Administration
Washington, DC 20546–0001

10. SPONSORING/MONITOR'S ACRONYM(S)

NASA

11. SPONSORING/MONITORING REPORT NUMBER

NASA/TM–20210021062

12. DISTRIBUTION/AVAILABILITY STATEMENT

Unclassified-Unlimited
Subject Category: 24
Availability: NASA STI Information Desk (757–864–9658)

13. SUPPLEMENTARY NOTES

Prepared by the Materials and Processes Laboratory, Engineering Directorate

14. ABSTRACT

Tailorability is one of the primary benefits offered by the use of polymer matrix composites (PMCs). However, real-world constraints often dictate that this tailorability is difficult to fully realize in practice. In flight hardware applications where components must be rigorously qualified, the prospect of tailoring a composite structure entails significant cost and schedule impacts given that each distinct composite layup family likely warrants some level of characterization. Thus, minimizing the number of composite layup families in a given application is often imperative. To this end, this study examines the use of non-traditional layups in the interest of establishing a more straightforward approach to tailoring in composite structures.

15. SUBJECT TERMS

polymer matrix composites, composite structures, tailoring, certification, modeling, optimization

16. SECURITY CLASSIFICATION OF:			17. LIMITATION OF ABSTRACT	18. NUMBER OF PAGES	19a. NAME OF RESPONSIBLE PERSON
a. REPORT	b. ABSTRACT	c. THIS PAGE			
U	U	U	UU	40	19b. TELEPHONE NUMBER *(Include area code)* STI Help Desk at: 757–864–9658

National Aeronautics and
Space Administration
IS02
George C. Marshall Space Flight Center
Huntsville, Alabama 35812